Soil Nonlinearity versus Frequency Effects

Wanda I. Cameron[1] and Russell A. Green[2]

Issue: Are observed trends in site amplification due to frequency effects being interpreted as soil non-linearity?

Prior to the 1989 Loma Prieta earthquake, there was an apparent disagreement among some geotechnical engineers and seismologists as to significance of soil non-linearity on observed ground motions. In essence, some seismologists found no evidence of soil non-linearity from recorded motions, with the exception of sites that experienced liquefaction (e.g., Aki, 1988). However, geotechnical engineers generally disagreed with this assessment, citing the trends shown in Figure 1. In this figure, the peak ground acceleration (pga) for non-rock sites are plotted as a function of the corresponding values for rock sites. The lower pga values for non-rock sites, relative to rock sites, was attributed to soil non-linearity by Seed et al. (1976).

After the Loma Prieta earthquake and subsequent data analyses, the seismologists capitulated, finding evidence of soil non-linearity in the recorded motions (Chin and Aki, 1991; Aki, 1993). Also, using data from the Loma Prieta and 1985 Mexico City earthquakes, as well as results from numerical site response analyses, Idriss (1990) developed the revised soft soil site amplification curve shown in Figure 2a. Although the trends shown in this figure, and by reciprocity the trends shown in Figure 1, have been attributed solely to soil non-linearity by many (e.g., NEHRP, 2001), Idriss (1991) showed that the trends are due to both soil non-linearity and frequency effects. This is illustrated in Figure 2b, wherein site amplification curves are shown for the same soft soil profile subjected to ground motions from M5.5 and M7 earthquakes scaled to different pga's. Idriss (1991) attributed the difference in the two curves to the frequency content of the ground motions -- the M5.5 ground motions were richer in high frequencies than the M7 motions.

Similar to Figure 2b, the frequency effects on site amplification can be seen in Figure 3, which was adapted from Chin and Aki (1991) and Aki (1993). In this figure, the horizontal axis is the mean of the peak accelerations ($pga_{observed}$) of the two horizontal components of motion recorded at a site. The vertical axis is the ratio of $pga_{observed}$ at a site and the mean pga predicted ($pga_{predicted}$) for the sites using appropriate source and path models, in conjunction with site amplification factors derived from weak motions using the coda method (Philips and Aki, 1986; Chin and Aki, 1991). The authors separated the sites into groups having hypocentral distances less than and greater than 50

[1] Doctoral Candidate, Department of Civil and Environmental Engineering, University of Michigan, Ann Arbor, MI
[2] Corresponding Author: Assistant Professor, Department of Civil and Environmental Engineering, University of Michigan, 2372 G.G. Brown Bldg, Ann Arbor, MI, 48109-2125, (734) 764-3668, rugreen@engin.umich.edu

km, which is roughly the near-field/far-field boundary proposed by Krinitzsky and Chang (1977) for a M7 earthquake (i.e., epicentral distance of 40 km). The basis for Krinitzsky and Chang's near field boundary was that the near field motions are considerably more erratic and richer in high frequencies than far field motions. It is clear from Figure 3, that the near-field sites experienced considerably less site amplification than the far field sites, which leads the authors to surmise that there is a significant frequency effect influencing the site amplification. [Note: The authors' interpretation of the data differs from that of Aki (1993), who attributes the noted trends to soil non-linearity.]

To further explore the influence of frequency content of ground motions on site amplification, a procedure for quantifying the characteristic period of the ground motion was needed. In this vein, various approaches proposed in literature were reviewed: Gutenberg and Richter (1956), Figueroa (1960), Seed et al. (1969), Shimazaki and Sozen (1984), and Rathje et al. (1998), as well as several others. For the purposes of this study, the index that appears to work the best is $T_{V/A}$ (Shimazaki and Sozen, 1984). $T_{V/A}$ is the period corresponding to the intersection of the constant spectral acceleration and velocity regions of a 5% damped Newmark-Hall type spectrum constructed using the actual *pga* and *pgv* values of a given ground motion, as shown in Figure 4. $T_{V/A}$ is computed by:

$$T_{V/A} = \frac{pgv}{pga} \cdot 2\pi \cdot \frac{\alpha_V(\xi = 5\%)}{\alpha_A(\xi = 5\%)} \quad (1)$$

where *pgv* = peak ground velocity. $\alpha_V(\xi = 5\%)$ and $\alpha_A(\xi = 5\%)$ are the median spectrum amplification factors for horizontal motion proposed by Newmark and Hall (1982) for the constant velocity and constant acceleration regions of 5% damped response spectra, respectively. $\alpha_V(\xi = 5\%) = 1.65$ and $\alpha_A(\xi = 5\%) = 2.12$. As noted by Shimazaki and Sozen (1984), $T_{V/A}$ coincides with the characteristic period defined in relation to the energy spectra, per Akiyama (1985).

A series of site response analyses were performed using a modified version of SHAKE91 (Idriss and Sun, 1992). The soft soil profile analyzed is shown in Figure 5 and is similar to the Redwood Shores profile, which was one of the profiles used by Idriss (1990) to develop the site amplification curve shown in Figure 2a. The input rock motions used in the analyses were the same ones used by Dobry et al. (1999) to develop the current NEHRP site response coefficients and were wide ranging in characteristics. The results of the analyses are shown in Figure 6. The horizontal axis in this figure is the ratio of the characteristic period of the ground motion ($T_{V/A}$) and the small strain fundamental period of the soil profile (T_n). The vertical axis is the ratio of the computed pga at the soil surface (pga_{soil}) and the pga of the input rock outcrop motion (pga_{rock}). The first series of analyses were performed holding the soil properties to their small strain values (i.e., no degradation or elastic - 5% damped). The results from this series of analyses are designated by open symbols in Figure 6. As may be observed from this figure, for the non-degrading profile the pga_{soil}/pga_{rock} increases as $T_{V/A}/T_n$ approaches one (i.e., resonance), as would be expected. The line fit to the non-degrading profile data delineates the upper limit of the frequency effects on site amplification.

Using the same soil profile and input motions, the site response analyses were repeated, only this time the soil properties were allowed to degrade from their small strain values. The results from this series of analyses are designated by filled symbols in Figure 6 and were grouped into three categories: pga_{rock} < 0.1g, which was comprised mostly of far field records; pga_{rock} = 0.1 – 0.2g, which was comprised of both far and near field records; and pga_{rock} > 0.2g, which was comprised entirely of near field records. [Note: The amplitudes of the input motions were not scaled.] A comparison of the lines fit to the data in these three categories allows the relative contributions of soil non-linearity and frequency effects to be discerned -- the vertical positions of the lines are functions of soil non-linearity and the slopes of the lines are functions of frequency effects. As may be observed from this figure, for the profile analyzed both soil non-linearity and frequency effects are significant for pga_{rock} < 0.2g, while soil non-linearity tends to dominate for pga_{rock} > 0.2g (as indicated by the relatively flat slope of the best fit line).

Additional analyses are being performed by the authors to better define the relative contributions of soil non-linearity and frequency effects for a wide range of soil profiles. However, from the analyses performed thus far, it is clear that in order reduce the uncertainty in the code specified ground motions the site classification system and corresponding site amplification factors need to account for both soil non-linearity and frequency effects. In a retrospective view of the soil non-linearity debate that occurred among some seismologists and geotechnical engineers, the inherent inter-relationship of soil non-linearity and frequency effects may have impeded the identification of soil non-linearity in the pre-Loma Prieta data and shrouded the significance of frequency effects in the post-Loma Prieta data.

Conclusion: Both soil non-linearity and frequency effects are important in site response analyses.

References:

Aki, K. (1988). Local Site Effects on Strong Ground Motion, Earthquake Engineering and Soil Dynamics II – Recent Advances in Ground Motion Evaluation (J.L. Von Thun, ed.), ASCE GSP 20: 103-155.

Aki, K. (1993). Local Site Effects on Weak and Strong Ground Motion, Tectonophysics, 218: 93-111

Akiyama, H. (1985). Earthquake-Resistant Limit-State Design for Building, University of Tokyo Press. 372pp.

Chin, B.-H. and K. Aki (1991). Simultaneous Study of the Source, Path, and Site Effects on Strong Ground Motion During the 1989 Loma Prieta Earthquake: A Preliminary Result on Pervasive Nonlinear Site Effects, Bulletin of the Seismological Society of America, 81(5): 1859-1884.

Dobry, R. (1991). Soil Properties and Earthquake Ground Response, Volume 4, Proceedings of the Tenth European Conference on Soil Mechanics and Foundation Engineering, Florence, Italy, May 26-30, 1991. 1171-1187.

Dobry, R., G.R. Martin, E. Parra, and A. Bhattacharyya (1999). Development of Site-Dependent Ratios of Elastic Response Spectra (RRS), Proc. Workshop on Earthquake Site Response and Seismic Code Provisions, University of Southern California, Los Angeles, CA, Nov. 18-20, 1992.

Figueroa, A. (1960). Some Consideration about the Effect of Mexican Earthquakes, Volume III, Proceedings: Second World Conference on Earthquake Engineering. 1553-1561.

Green, R.A. and W.I. Cameron (2003). The Influence of Ground Motion Characteristics on Site Response Coefficients, Proc., 7th Pacific Conf. on Earthquake Engineering, University of Canterbury, Christchurch, New Zealand, Feb. 13-15, Paper Number 90, 8pp.

Gutenberg, B. and C.F. Richter (1956). Earthquake Magnitude, Intensity, Energy, and Acceleration (Second Paper), Bulletin of the Seismological Society of America. 46(2). 105-145.

Idriss, I.M. (1990). Response of Soft Soil Sites During Earthquakes, Volume 2, Proceedings: H. Bolton Seed Memorial Symposium, (J.M. Duncan, ed.), University of California, Berkeley, May 1990. 273-289.

Idriss, I.M. (1991). Earthquake Ground Motions at Soft Soil Sites, Proc. 2nd Int. Conf. on Recent Advances in Geotechnical Earthquake Engineering and Soil Dynamics, March 11-15, St. Louis, Missouri, 2265-2272.

Idriss, I.M. and J.I. Sun (1992). SHAKE91: a computer program for conducting equivalent linear seismic response analyses of horizontally layered soil deposits, University of California, Davis.

Krintizsky, E.L. and F.K. Chang (1977). Specifying Peak Motions for Design Earthquakes, State-of-the-Art for Assessing Earthquake Hazards in the United States, Report 7, US Army Engineer Waterways Experiment Station, Vicksburg, MS.

NEHRP (2001). NEHRP Recommended Provisions for Seismic Regulations for New Buildings and Other Structures, Part 1- Provisions: FEMA 368, Part 2-Commentary FEMA 369, Federal Emergency Management Agency, Washington DC.

Newmark, N.M. and W.J. Hall (1982). Earthquake Spectra and Design, Earthquake Engineering Research Center, Oakland, CA, 103pp.

Phillips, W.S. and K. Aki (1986). Site Amplification of Coda Waves from Local Earthquakes in Central California, Bulletin of the Seismological Society of America, 76(3): 627-648.

Rathje, E.M., N.A. Abrahamson, and J.D. Bray (1998). Simplified Frequency Content Estimates of Earthquake Ground Motions, Journal of Geotechnical and Geoenvironmental Engineering. 124(2). 150-159.

Seed, H.B., I.M. Idriss, and F.W. Kiefer (1969). Characteristics of Rock Motions During Earthquakes, ASCE Journal of the Soil Mechanics and Foundation Division. 95(5). 1199-1218.

Seed, H.B. and I.M. Idriss (1983). Ground Motions and Soil Liquefaction During Earthquakes, EERI Monograph, Earthquake Engineering Research Institute, Oakland, CA.

Seed, H.B., R. Murarka, J. Lysmer, and I.M. Idriss (1976). Relationships of Maximum Acceleration, Maximum Velocity, Distance from the Source, and Local Site Conditions for Moderately Strong Earthquakes, Bulletin of the Seismological Society of America, 66(4): 1323-1342.

Shimazaki, K. and M.A. Sozen (1984). Seismic Drift of Reinforced Concrete Structures. Special Research Paper (Draft). Hazama Corp.

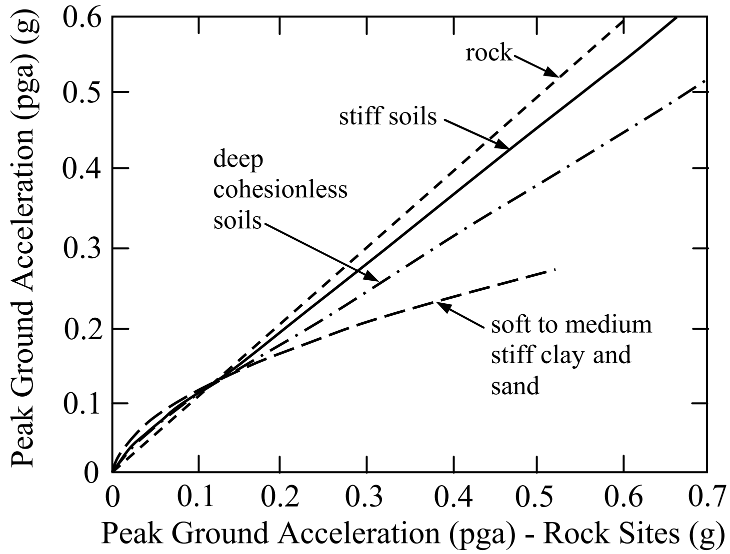

Figure 1. Site amplification curves for varying soil profiles. The trends shown in these curves have been attributed solely to soil non-linearity. (Adapted from Seed et al., 1976 and Seed and Idriss, 1983)

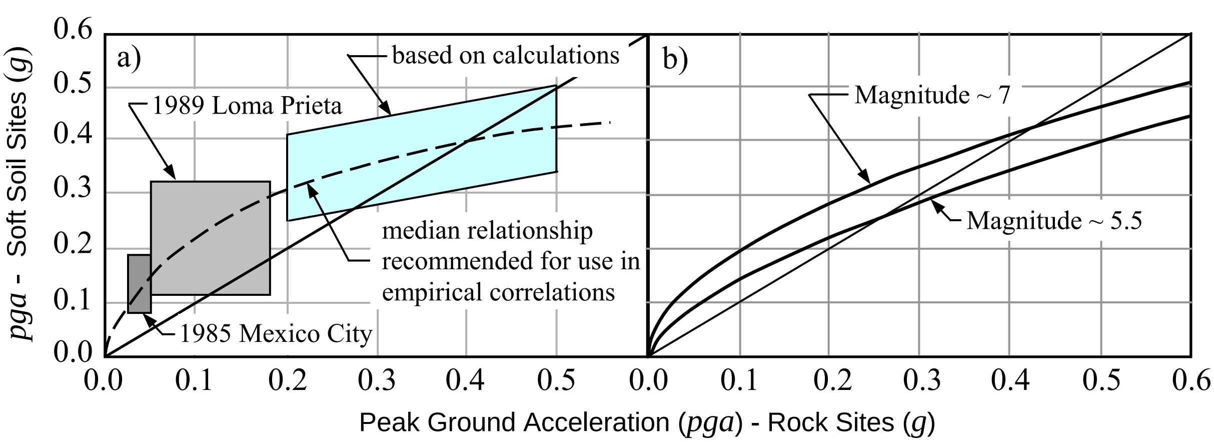

Figure 2. a) Soft soil site amplification curve developed from observed data from the the Loma Prieta and 1985 Mexico City earthquakes, as well as numerical site response analyses. (Adapted from Idriss, 1990). b) Soft soil site amplification curves developed using acceleration time histories from M5.5 and M7 earthquakes scaled to different pga's. The difference in these two curves is attributed to frequency effects. (Adapted from Idriss, 1991).

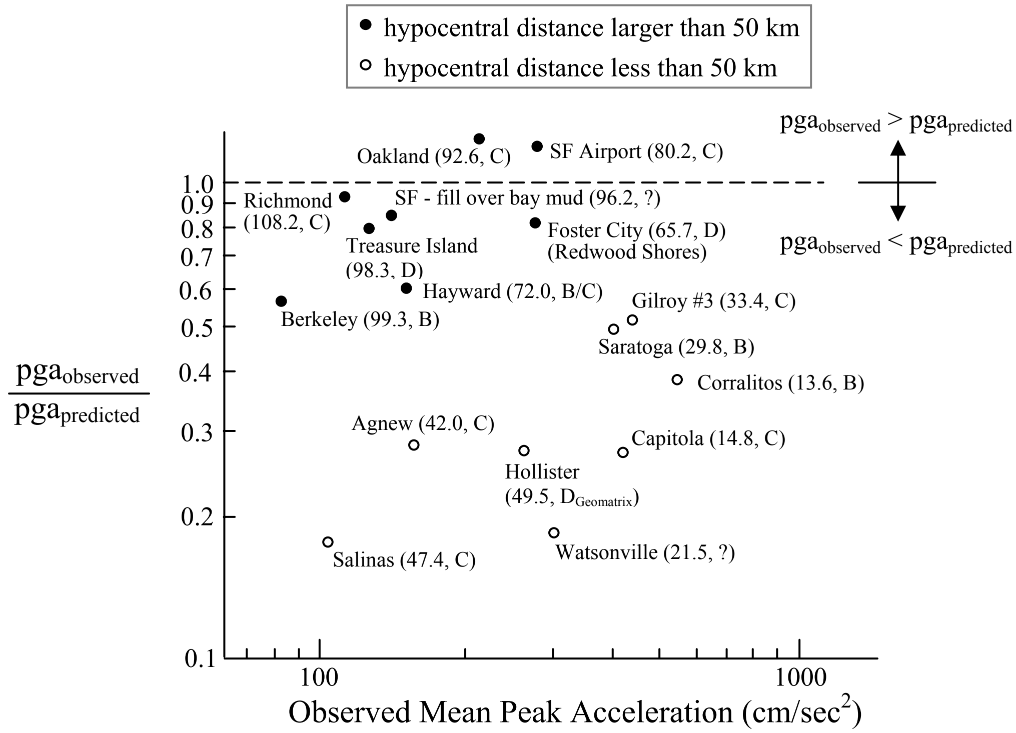

Figure 3. Ratio of observed and predicted pga's from various soil sites subjected to shaking during the Loma Prieta earthquake. Next to each point is the seismograph station name, and in the parentheses next to the station name are the hypocentral distance and the USGS site classification. (Adapted from Chin and Aki, 1991 and Aki, 1993)

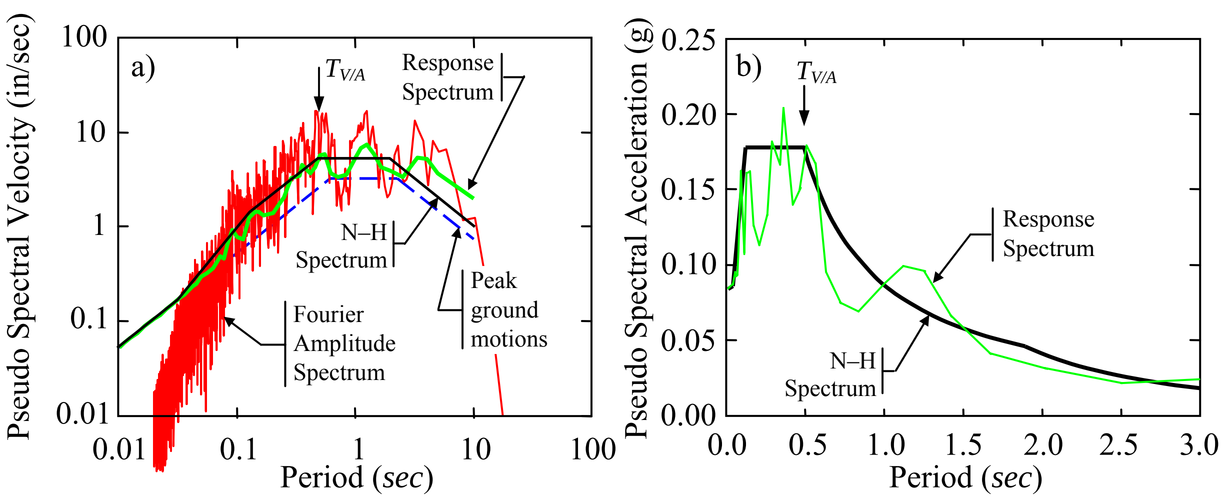

Figure 4. Definition of the $T_{V/A}$ which was used to defined the characteristic period of the earthquake ground motions. a) Defined with respect to the pseudo velocity spectrum on tripartite log paper (Fourier amplitude spectrum shown for comparison only). b) Defined with respect to the pseudo acceleration spectrum. (Adapted from Green and Cameron, 1993)

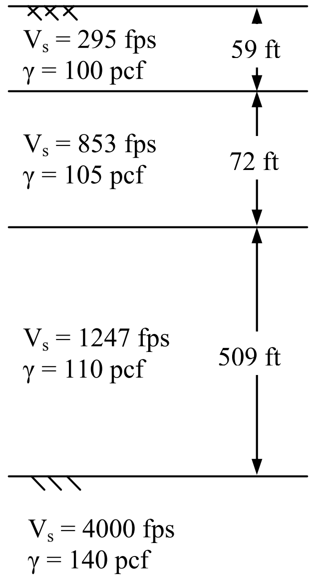

Figure 5. Soft soil profile used in the site response analyses to generate the data presented in Figure 6. This profile is similar to the Redwood Shores profile, which was one of the profiles used to generate the soft soil amplification curve in Figure 2a.

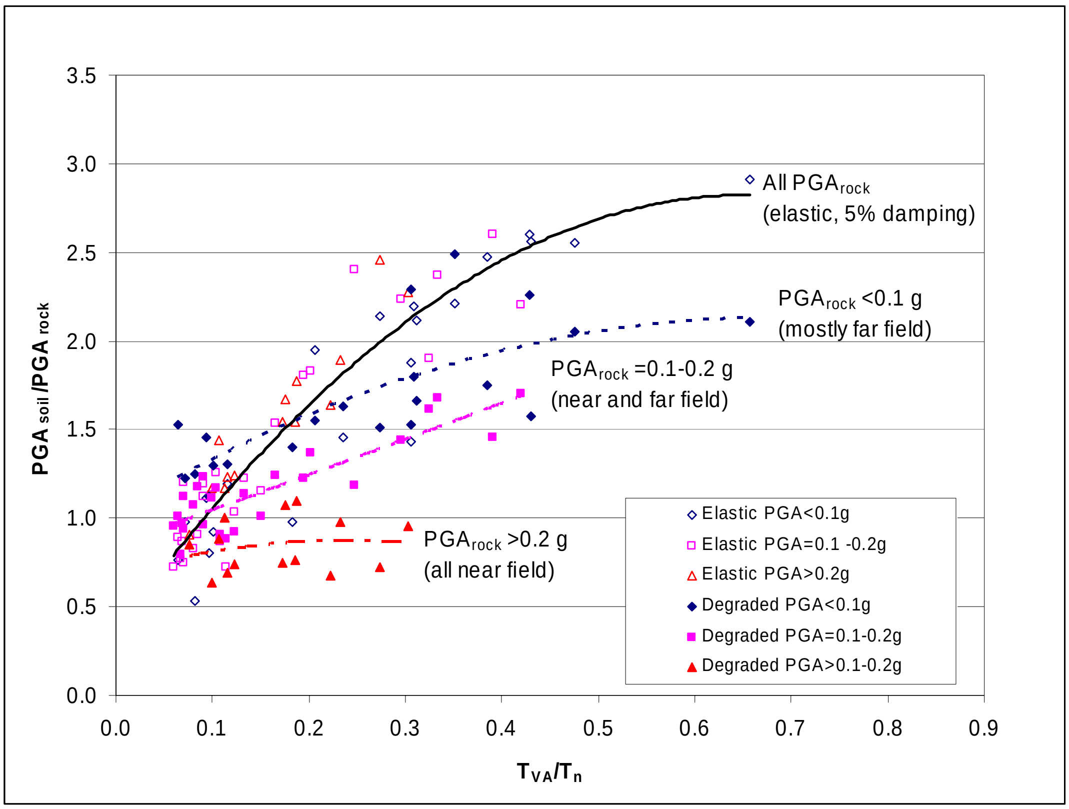

Figure 6. The results from a series of site response analyses performed on the soft soil profile shown in Figure 5. The open symbols are from analyses wherein the soil properties were held at their small strain values. The filled symbols are from analyses that allow the soil properties to degrade. The vertical positions of the best fit lines are functions of soil non-linearity, while the slopes of the lines are functions of frequency effects.